NJC

Accepted Manuscript

This is an *Accepted Manuscript*, which has been through the Royal Society of Chemistry peer review process and has been accepted for publication.

Accepted Manuscripts are published online shortly after acceptance, before technical editing, formatting and proof reading. Using this free service, authors can make their results available to the community, in citable form, before we publish the edited article. We will replace this *Accepted Manuscript* with the edited and formatted *Advance Article* as soon as it is available.

You can find more information about *Accepted Manuscripts* in the Information for Authors.

Please note that technical editing may introduce minor changes to the text and/or graphics, which may alter content. The journal's standard Terms & Conditions and the Ethical guidelines still apply. In no event shall the Royal Society of Chemistry be held responsible for any errors or omissions in this *Accepted Manuscript* or any consequences arising from the use of any information it contains.

ROYAL SOCIETY OF CHEMISTRY

www.rsc.org/njc

Anti-inflammatory properties of Au-scopoletin Nanoconjugates

Muhammad Raza Shah[1,*], Anwar Shamim[1], Lauren S. White[2], Massimo F. Bertino[2], M. Ahmed Mesaik[3] Samreen Soomro[1]

[1]H.E.J. Research Institute of Chemistry, International Center for Chemical and Biological Sciences, University of Karachi, Karachi-75270, Pakistan.

[2]Department of Physics, Virginia Commonwealth University, Richmond, VA 28234, USA

[3]Universiti Kebangsaan Malaysia (UKM), the National University of Malaysia Kuala Lumpur Malaysia

ABSTRACT

We investigated the biological activity of Au nanoparticles with a mean diameter of 30 nm which were capped with scopoletin, a natural coumarin isolated from *Artemisia roxburghiana* along with eleven other natural products. The NO inhibitory activity of scopoletin was unaffected by conjugation to the Au nanoparticles. Luminol chemiluminescence assay showed instead that conjugation increased the prevention of oxidative burst of reactive oxygen species (ROS) in whole blood phagocytes and isolated neutrophils (PMN) by about three times.

***Correspondence:**

Dr. Muhammad Raza Shah

H.E.J. Research Institute of Chemistry, International Center for Chemical and Biological Sciences, University of Karachi, Karachi-75270, Pakistan

e-mail: raza.shah@iccs.edu

Ph: +92 (21) 111 222 292 ext 233

fax: +92 (21) 34819018.

1. Introduction

There is considerable evidence showing that Au nanoparticles are typically biologically inert.[1] Several studies have consistently demonstrated that while Au nanoparticles can enter cells,[2,3] typically via phagocytosis,[4,5] they do not appear to alter cell metabolism[6]. In contrast, conjugation to Au nanoparticles does increase the potency of several therapeutic agents. For example, increased anti-inflammatory activity of Au nanoparticle conjugates has been demonstrated.[7] The group of Kotov showed that conugates of Au nanoparticles and mercaptopurine were very efficient in antiproliferation against leukemia due to enhanced delivery.[8] Au nanoparticles conjugated with epigallocatechin and α-lipoic acid can also facilitate healing by reducing inflammation in muscle injury[9] and in diabetic wounds.[10] The present work includes isolation of twelve compounds (Figure 1) including four triterpenes, two flavones, two coumarins, one sterol glycoside, two fatty acids, and one alcohol called Lupeol (**1**), Taraxeryl acetate (**2**), Betulin (**3**), Betulinic acid (**4**), Apigenin-7, 4-dimethyl ether (**5**) 7-hydroxy-4-methoxy-flavone (**6**), Scopoletin (**7**), 6-7 dimethoxy coumarin (**8**), ß-Sitosterol Glucoside (**9**), Stearic acid (**10**), Docosanoic acid (**11**), and n-nonacosanol (**12**). Compounds **1-8** were obtained for the first time from *Artemisia roxburghiana*. Scopoletin (**7**) was capped around gold nanoparticle and its anti-inflammatory activity was compared with that of uncapped Au nanoparticles.

Pure scopoletin and Au-scopoletin conjugates had a comparable NO inhibiting activity; however, conjugates were about 3 times more efficient than pure scopoletin in preventing the oxidative burst induced by reactive oxygen species (ROS) in phagocytes and isolated neutrophils.

Our results indicate that conjugation to Au nanoparticles does not inhibit the potency of scopoletin but at the same time the potency is not automatically increased by conjugation in case of NO inhibition. Increased potency of nanoconjugates with respect to ROS should therefore not be regarded as an automatic consequence of conjugation, but it should be verified by thorough and critical biological and clinical testing.

2. Experimental

2.1. Materials and instruments

Reagent grade Tetrachloroauric acid trihydrate ($HAuCl_4 \bullet 3H_2O$), methanol, ethanol, butanol, hexane, ethyl acetate and sodium borohydride were purchased from Merck. UV-Vis spectra were recorded with a Schimadzu UV-240 spectrometer with a path length of 1 cm. FT-IR spectra were recorded using a Shimadzu IR-460. The ^1H NMR spectra were recorded on a Bruker spectrometer (400 MHz, $CDCl_3$) and ^{13}C NMR spectra were also recorded on a Bruker spectrometer (125 MHz, $CDCl_3$) using TMS as an internal standard and $CDCl_3$ as solvent. Transmission electron microscopy was carried out using a Zeiss Libra 120 operated at 120 keV in STEM mode. GCMS measurements were taken using a JEOL JMS 600-H with helium gas, column ZB-5MS.

2.2. Isolation of scopoletin from Artemisia roxburghiana

Scopoletin along with four triterpenes, two flavones, one coumarin, one sterol glycoside, two fatty acids, and one alcohol were isolated from *Artemisia roxburghiana* by column chromatography. Shade- dried powder of the whole plant of *Artemisia roxburghiana* (17 kg) was soaked in methanol three times for better extraction. The methanolic extract was concentrated by evaporation in vacuum and then was portioned into various fractions (Hexane, Ethyl acetate, Butanol, and Water), as shown in Scheme 1. About 150 g of the ethyl acetate fraction was loaded on a glass column (120cm×10cm) previously packed with silica gel (500 g) in hexane. The extract was gradiently eluted with hexane containing an increasing proportion of ethyl acetate. Crystals of Scopoletin (50mg) were obtained at polarity 4:6 (Ethyl acetate: Hexane) in impure form and they were further purified by washing with methanol. The structure of scopoletin was established on the basis of ^1H NMR, ^{13}C NMR and Mass spectrometry.

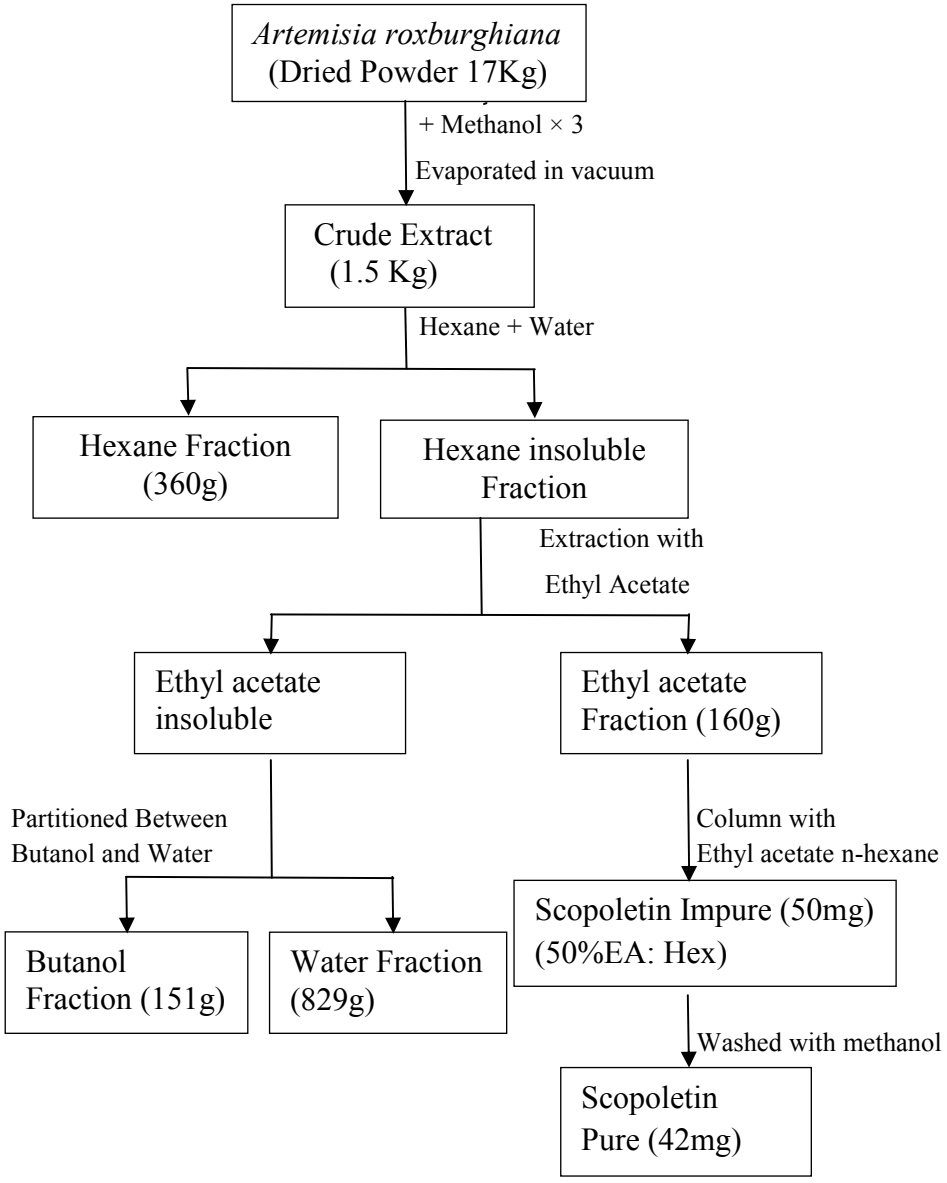

Scheme 1: Isolation of scopoletin from *Artemisia Roxburghiana*

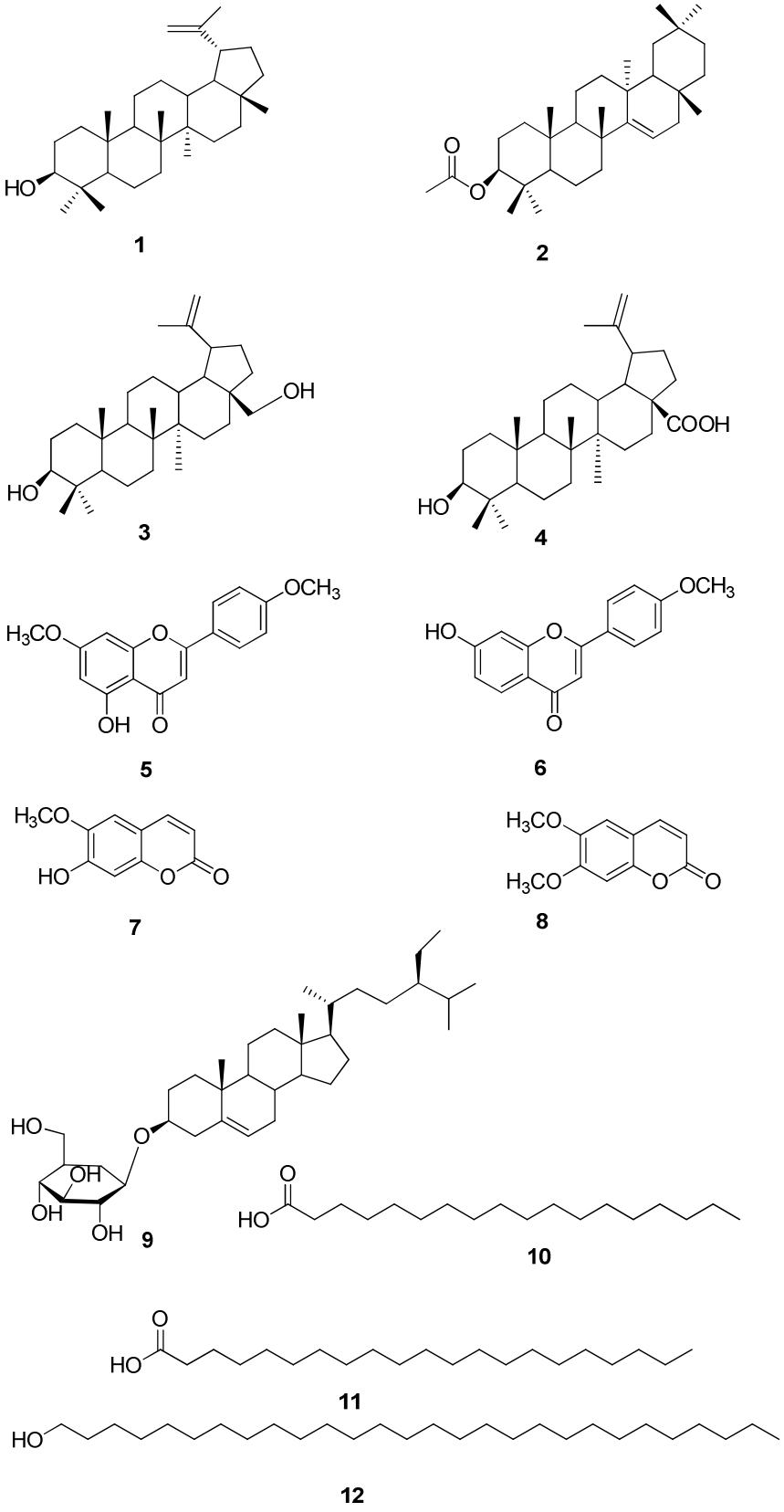

Figure 1: Structures of isolated compounds from *Artemisia roxburghiana*

2.3. NMR data of isolated compounds including scopoletin:

The ^{1}H-NMR spectrum of scopoletin displayed a pair of doublets in the aromatic region (δ value 7.5 and 6.2) with one proton integration each and a coupling constant of J = 9.3 Hz. Two singlets at δ 6.8, δ 6.0 were assigned for methine two protons. Signals at δ 3.9 were attributed to the methoxy proton. ^{13}C NMR spectrum revealed the presence of ten carbons including one methoxy, four methines and five quaternary carbons. Signals for aromatic carbon appeared at δ 113.4 and δ 143.2. A signal at δ 56.3 confirmed the presence of methoxy carbon in the molecule. Table-1 shows the detailed ^{1}H NMR and ^{13}C NMR data for scopoletin which is in agreement with data in the literature.[11]

Other isolated compound from *Artemisia roxburghiana*, including Lupeol (**1**),[12] Taraxeryl acetate (**2**),[13] Betulin (**3**),[14] Betulinic acid (**4**),[15] Apigenin-7, 4-dimethyl ether (**5**),[16] 7-hydroxy-4-methoxy-flavone (**6**),[17] Scopoletin (**7**),[11] 6-7 dimethoxy coumarin (**8**),[11] ß-Sitosterol Glucoside (**9**),[18] Stearic acid (**10**),[19] Docosanoic acid (**11**),[20] and n-nonacosanol (**12**),[21] were also characterized through spectroscopic and spectrometric techniques, and the associated data was compared to data in the literature and was seen to be quite similar.

Carbon. No	Multiplicity (DEPT)	δ_C	δ_H	J_{HH} (Hz)
C-2	C	δ 161.4	-	-
C-3	CH	δ 113.4	6.2	d (9.2)
C-4	CH	δ 143.2	7.5	d (9.6)
C-5	CH	δ 107.4	6.8	d (9.2)
C-6	C	δ 143.2	-	-
C-7	C	δ 149.6	-	-
C-8	CH	δ 103.1	6.0	S

C-9	C	δ 150.2	-	-
C-10	C	δ 111.4	-	-
6-OMe	CH3	δ 56.3	3.9	S

Table 1: ^{13}C NMR and ^{1}H NMR spectral data of scopoletin

2.4. Synthesis of gold scopoletin capped nanoparticles

Because scopoletin has very low solubility in water, it was dissolved in methanol. 1mL of scopoletin-methanol solution (1mM) was slowly added to 4 mL of Tetrachloroauric acid trihydrate (1mM) followed by the addition of 0.4mL of Sodium borohydride solution (1mM) after 20 minutes while stirring. The reaction was carried out under stirring at room temperature for 4 hours. In most experiments, a 4:1 mole ratio of Au to scopoletin was used which yielded suspensions with an absorption maximum λ_{max} at 528 nm as shown in Figure 2.

2.5. Bioassays of scopoletin and its gold nanoparticles

2.5.1. Immunomodulatory activity

Heparinized blood was obtained by vein puncture aseptically from healthy volunteers (25–38 years old). The Buffy coat containing (PMNs) was collected by dextran sedimentation and the cells were isolated with density gradient centrifugation from the lymphocyte separation medium (LSM, purchased from MP Biomedicals). PMNs were collected from the tube base. Neutrophils were purified from red blood cells (RBCs) contamination using a hypotonic solution. Cells were washed twice and suspended in a Ca^{++} and Mg^{++} free Hank's Balance Salt Solution (HBSS--), after which the pellet was obtained by centrifugation and cells were adjusted to their required concentration using Hank's Balance Salt Solution containing Ca^{++} and Mg^{++} (HBSS++). The Hank's balance salts solution (HBSS) was purchased from Sigma (St. Louis, MO, USA).

2.5.2. Chemiluminescence Assay

Luminol enhanced Chemiluminescence's assay was performed in white half area 96 well plates [Costar, NY, USA],[22]. Three concentrations of compounds (1, 10 and 100 µg/mL) were added and incubated at 37 ºC for 15 minutes in the thermostat chamber of a luminometer [Labsystems, Helsinki, Finland] with whole blood (1:20 dilution in sterile HBSS++), phagocytes, or isolated neutrophils (1 x 106 cells/mL). The negative control wells received HBSS++ and cells but no compounds. After incubation, intracellular reactive oxygen detecting probe luminol [Research Organics, Cleveland, OH, USA], working solution (7 x 105 M), and serum opsonized zymosan (SOZ) 2 mg/mL [Fluka, Buchs, Switzerland] were added into each well, except for the blank wells which contain only the HBSS++. The oxidative burst ROS production was monitored with the luminometer for 50 minutes in the repeated scan mode. The level of the ROS was recorded as total integral readings ain relatively light units (RLU) using Lab systems Luminoskan RS (MTX Lab Systems, Inc. Vienna, Virginia)

2.5.3. Nitrite concentration in Mouse Macrophage Culture Medium

The mouse macrophage cell line J774.2 (European Collection of Cell Cultures, Salisbury, UK) was cultured in 75 cc flasks (IWAKI Asahi Techno Glass, Tokyo, Japan) in DMEM (Sigma-Aldrich Steinheim, Germany) that contained 10% fetal bovine serum (GIBCO New York U.S) supplemented with 1% streptomycin/penicillin. Flasks were kept at 37°C in humidified air containing 5% CO_2. Cells (106 cells/mL) were then transferred to a 24-well plate. The nitric oxide synthase (NOS-2) in macrophages was induced by the addition of 30 µg/mL of *E.coli* lipopolysaccharide (LPS) (DIFCO Laboratories Michigan, USA). The test compounds were added at 25 µg/mL concentration, and shortly after the LPS stimulation, the cells were again incubated at 37°C in 5% CO_2. The cell culture supernatant was collected after 48 hours for analysis. Nitrite accumulation in the cell culture supernatant was measured using the Griess method. 50 µl of 1% sulphanilamide in 2.5% phosphoric acid, followed by 50 µl of 0.1% naphtyl-ethylene diamine dihydrochloride in 2.5% phosphoric acid was added to 50 µl of culture medium. After 10 minutes of incubation at room temperature the absorbance was read at 550 nm. Micro molar concentrations of nitrite

were calculated from a standard curve generated using sodium nitrite which was used as reference compound.

2.5.4. Statistics

The values are expressed as means ± SD. The significance of difference from the respective controls for each experimental test condition was assayed by using one way ANOVA and student T test for each paired experiment. P value <0.05 was regarded as indicating significant differences and denoted as* while p<0.005 was denoted as**.

3. Results and Discussion

Scopoletin was isolated from *Artemisia Roxburghiana* by column chromatography as described in the Experimental Section. To alleviate solubility issues, scopletin was dissolved in methanol and then added to an aqueous solution of $HAuCl_4$. Au ions were reduced using $NaBH_4$ as described in the Experimental Section. Following characterization, the activity of the conjugates for biologically relevant processes such as NO inhibitory activity and inhibition of oxidative burst of reactive oxygen species (ROS) was investigated.

3.1. Synthesis and characterization of Gold nanoparticles

Addition of $NaBH_4$ solution resulted in a change of color from light yellow to dark pink indicating reduction of Au+ ions and formation of gold nanoparticles. The UV-Visible spectrum of this colloidal solution is reported in Figure 2, and it exhibits an absorption maximum at 528 nm. The measurements are in accordance with the literature where it has been shown that aqueous solutions of spherical gold nanoparticles have absorption maxima between 520 to 530nm.[23]

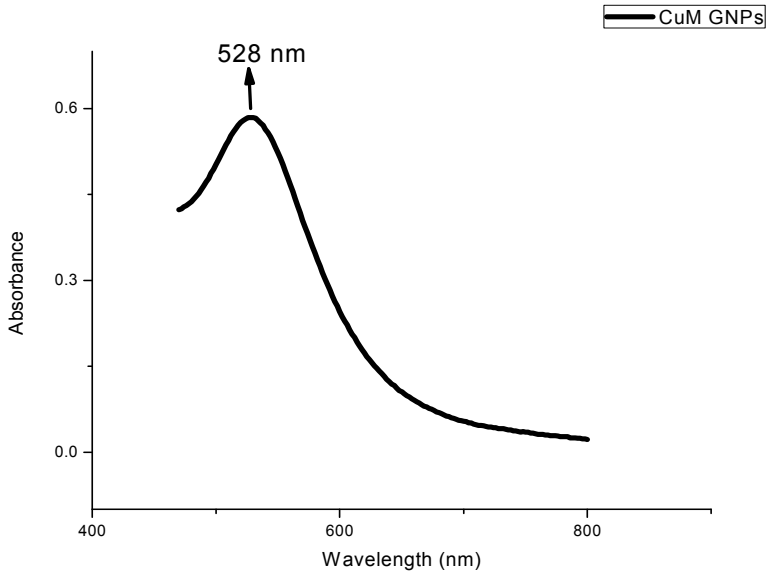

Figure 2: UV–Vis spectrum of gold nanoparticles stabilized with scopoletin.

The FTIR spectrum of scopoletin provided in Figure 3 shows clear peaks in the –O-H, C=O and C-O stretching regions at 3335 cm^{-1}, 1703 cm^{-1}, and 1291cm^{-1} respectively. Peaks at 1511 cm^{-1}, 1566 cm^{-1}, and 1608 cm^{-1} were attributed to the aromatic C=C stretch. Several peaks between 1300 and 1465 cm^{-1} were also measured which could be reconciled with the C-H stretch of methyl groups. Methoxy C-O, phenolic C-O, C-O of ester group and C-O of aryl ester group were responsible for the peaks at 1291cm^{-1}, 1263cm^{-1}, 1140 cm^{-1}, and1017 cm^{-1}, respectively. Peak shifting, weakening[24] and disappearance[25] are expected for functional groups interacting with the gold nanoparticles. Most of the peaks in the FTIR spectrum of scopoletin stabilized GNPs are very weak (O-H and C=O peaks) with some peaks almost disappeared in the region 1000-1600 cm^{-1}. This indicates that these functional groups (OH, C=O, C-C and aromatic C=C) are probably interacting with the metal (Au) in the nanoparticles. On the other hand the peaks due to the stretching of $–CH_3$ groups are the same in both spectra indicating no prominent role of these groups in the interaction with GNPs. Thus, the IR spectrum indicates that the aromatic system, carbonyl groups, hydroxyl groups, as well as methoxy groups are involved in the stabilization of gold nanoparticles.

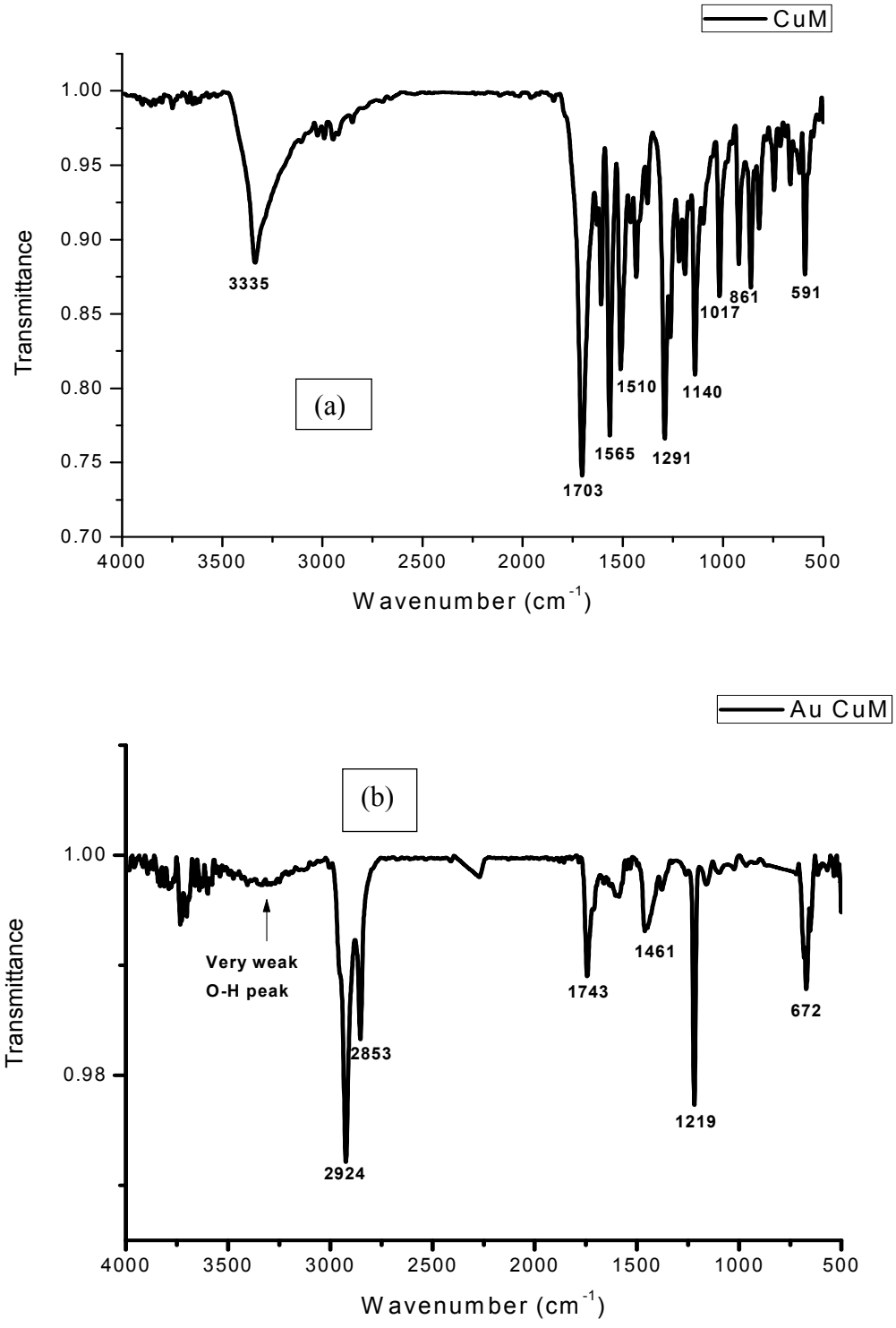

Figure 3: (A) FT-IR spectrum of scopoletin (B) FT-IR Spectrum of scopoletin-GNP conjugates.

Transmission electron microscopy analysis was carried out in both STEM and TEM mode. Representative images are reported in Figures 4 and 5 and they show that the nanoparticles were polydisperse with sizes ranging from about 5 to 25 nm. Selected area diffraction (SAED) is reported in the inset of Figure 5. Diffraction rings are well-evident and they show that the particles are crystalline with a fcc structure.[26]

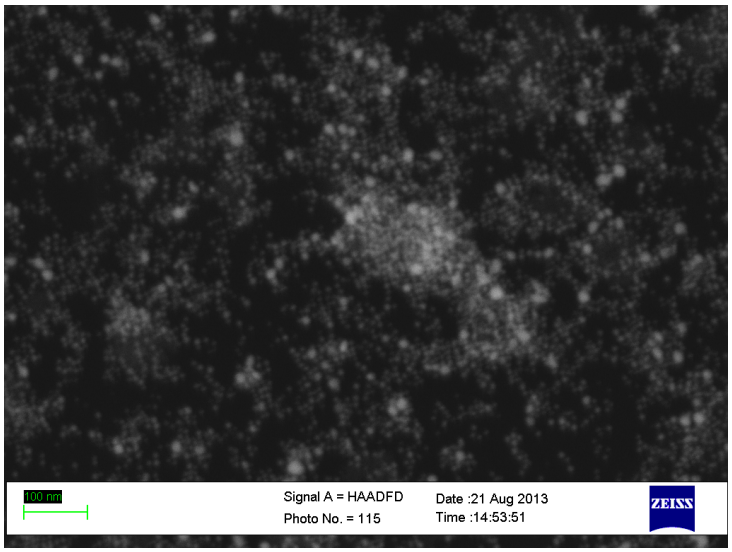

Figure 4: STEM image of scopoletin-GNP conjugates.

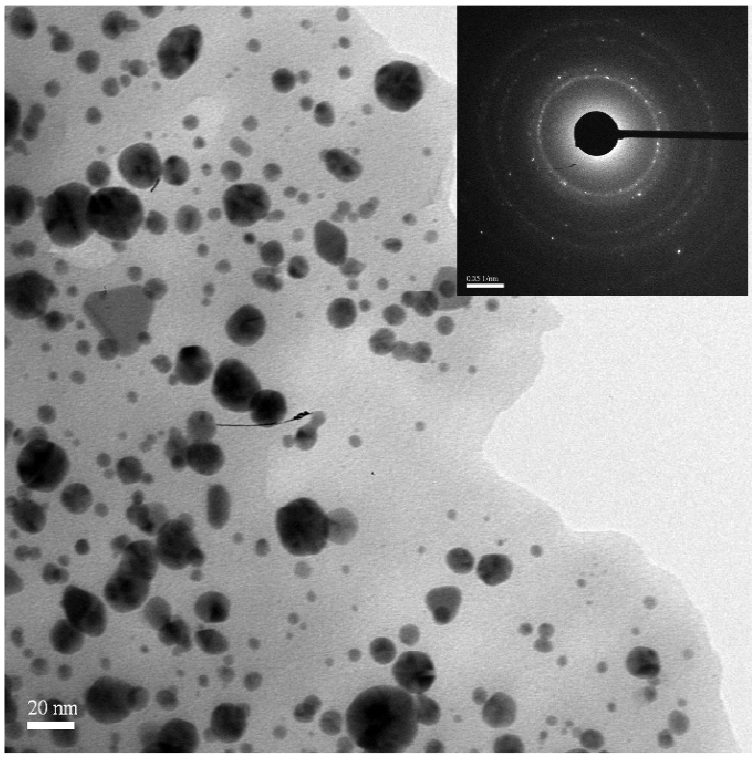

Figure 5: Bright field transmission electron micrograph showing Au nanoparticles. The inset shows a selected area diffraction (SAED) image proving that the particles have a fcc crystalline structure. [26]

To investigate the behavior of the nanoparticles under physiological conditions, temperature and salt concentrations of the suspensions were varied. Figure 6 shows the effect of pH on stability of GNPs. The nanoparticles showed resistance within a pH range 2-12 but precipitation is observed below pH 2 and above pH 12 which is confirmed by UV-Visible absorption Spectra as shown in the Figure 6.

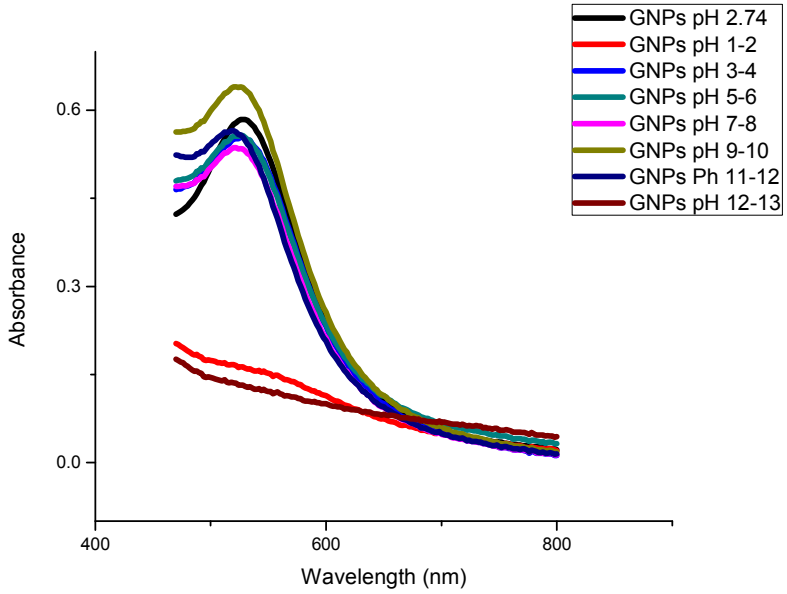

Figure 6: Effect of pH change on the stability of GNPs.

Figure 7 shows the effect of heat on the stability of gold nanoparticles. GNPs were heated at 100 ^{o}C for 5 minutes and were found to slowly precipitate as indicated by the quenching of peak in the UV spectrum. This effect can be attributed to the dominant electronic dephasing mechanism which involves electron-electron interaction, as higher electronic temperatures do not only lead to a faster electron-electron scattering rate but also increase the electron-surface and electron-defect scattering. The velocity of an electron depends on its state energy and hence on the temperature; the velocity rises for higher excited electronic states. Since an increase in the velocity of the electrons leads to a larger damping constant and therefore to a faster dephasing, this results in the reduction of absorbance of the Plasmon band.[27]

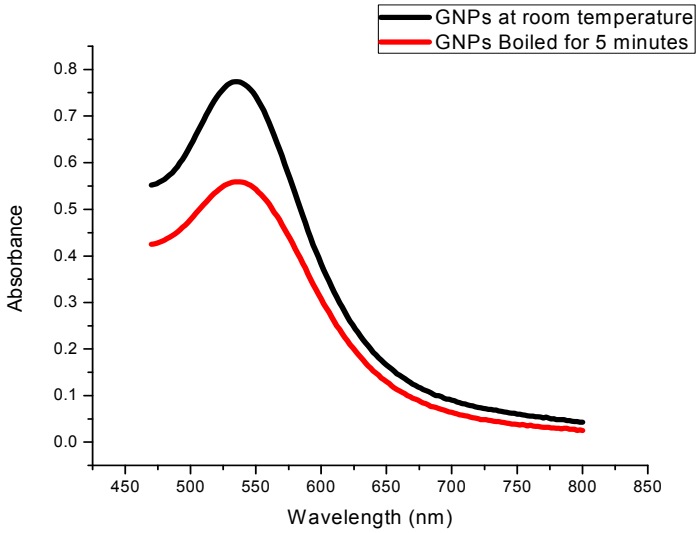

Figure 7: Effect of heat on stability of GNPs.

Figure 8 shows the effect of Brine solutions of different concentrations ranging from 0.1M to 5M on scopoletin stabilized gold nanoparticles. The data shows that quenching occurred as the concentration of salt solution increases. This quenching can be attributed to the fact that the molar concentration and valence of destabilizing counter ion i.e. Na^+ screens the effective surface charge and repulsive force between the electrostatically stabilized nanoparticle suspensions[28]. This may lead to destabilization of nanoparticles and trigger aggregation.

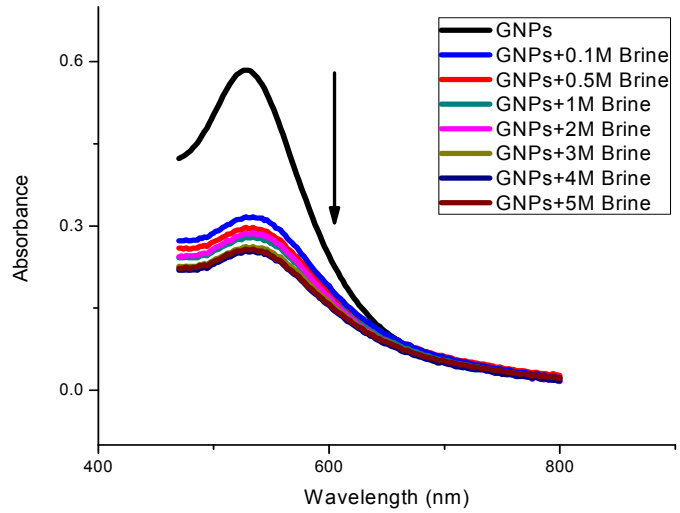

Figure 8: Effect of Brine solution on stability of GNPs.

3.2. Amount of coumarin conjugated with Au nanoparticles:

To quantify the activity of the conjugates, the amount of scopoletin adsorbed on the nanpoarticles' surface had to be determined. For this, a freshly prepared suspension of GNPs from 12mL (5mM) of tetrachloroauric acid trihydrate and 3 mL of scopoletin (5mM) was centrifuged. After centrifugation the supernatant was removed. The solid remaining in the tube was dried and its mass was found to be 9.7 mg. This weight included scopoletin adsorbed onto the Au nanoparticles. UV-Visible spectroscopy (Figure 9) showed that the supernatant did not contain any nanoparticles or scopoletin. GC-MS analysis confirmed that scopoletin was not present in the supernatant. Since 2.88 mg of scopoletin were used for the synthesis, and none was found in the supernatant, we conclude that the scopoletin content of the conjugates was 2.88 mg, or about 29.7% of the total weight (9.7 mg).

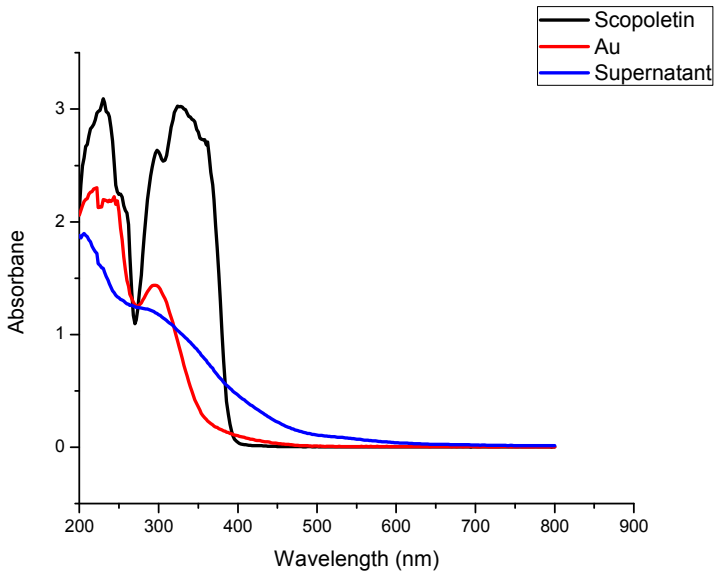

Figure 9: UV-Vis spectra of pure scopoletin, gold solution, and supernatant obtained after centrifugation.

S#	Compounds	% NO inhibition	IC_{50} (µg/mL)	
			Whole blood ROS	Neutrophils ROS
1	GNPs	21.6	51.3 ± 1.8	1.1 ± 0.1
2	Scopoletin	78.8	4.6 ± 0.3	0.8 ± 0.1
3	**Ibuprofen**	**ND**	**11.2 ± 1.9**	**2.5 ± 0.6**
4	**LNMA**	**65**	-	-
5	Bare-GNP	10.1	61.4± 1.9	2.1 ± 0.3

Table 2: Effect of scopoletin and its GNPs on the whole-blood and PMNs oxidative burst, activated by SOZ. The IC_{50} values were calculated using various doses of each compound. Ibuprofen was used as positive control in oxidative burst assay, whereas N^G Monomethl L-Arginine Acetate's (LNMA) NO inhibitor $p<0.005$ ** and <0.05* properties are calculated using ANOVA test. ND: not determined.

3. 3. Biological Evaluation

The biological activity of scopoletin and its conjugates was tested as described in the experimental section and the results are reported in Table-2. Scopoletin showed significant ($p \leq 0.005$) inhibition of NO production in the J774 cells. The inhibition was 78% by Scopoletin and 21.6% for the Au nanoparticle conjugates. Since the amount of scopoletin adsorbed to the GNPs is 29.7% by weight, we can conclude that the NO inhibition of the conjugates per unit weight of scopoletin is $\frac{21.6\%}{29.7\%} \cong 72.7\%$, which is comparable to that of pure scopoletin.

Reactive oxygen species were also equally suppressed by scopoletin and its gold conjugates. Considering the actual amount of scopoletin attached to the Au nanoparticles (29.7%), the suppression with GNPs is almost three times higher than that of pure scopoletin.

4. Conclusion

In this work we have investigated the activity of scopoletin conjugated to Au nanoparticles against two relevant biological processes, nitric oxide inhibition and oxidative burst of reactive oxygen species. Our goal was to determine whether conjugation increased the activity of scopoletin. Based on our previous work on conjugation of antibiotics and antioxidants to Au and Ag nanoparticles, we expected an increased activity of scopoletin.

Biological systems were treated with the same amount of scopoletin and Au-scopoletin conjugates, and the activities of the conjugates were lower than that of pure scopoletin. Once the results were corrected for the amount of scopoletin contained in the conjugates, a fraction of the total weight, the activity of the conjugates was higher than that of scopoletin for reactive oxygen species. Conjugation did not affect the nitric oxide inhibitory activity. Our results show, therefore, that conjugation to nanoparticles is not detrimental to the activity of the attached molecules; however, enhancement of the activity depends on the targeted pathology and biological system.

Acknowledgements

We are grateful to COMSTECH-TWAS No:11-109 RG/MSN/AS_C-UNESCO FR: 3240262659 and Higher Education Commission project number 20-616/R&D/2006/ of Pakistan for the financial support.

References

1. R. Shukla, V. Bansal, M. Chaudhary, A. Basu, R.R. Bhonde and M.B. Sastry. *Langmuir*. 2005, 21(23), 10644-10654.
2 P.O.C. Chen, C. Sandra, M. Adegboyega and K. Oyelere *Nanotechnology, Science and Applications* 2008, 1, 45–66
3 H. Hillaireau, and P. Couvreur. *Cellular* and *Molecular Life Sciences* 2009, 66, 2873-2896
4 Y. Wang, B. Wang, Mo-Tao Zhu. M. Li, H-J, Wang, M. Wang, H. Ouyang, Z-F. Chai. W-Y. Feng. and Y-L. Zhao *Toxicology Letters*, 2011, 205(1), 26–37
5 J.K. Seung and I.H.C. Yonsei *Medicinal Journal* 2012, 53(3), 654-657.
6 E. E. Connor, J. Mwamuka, A. Gole, C. J. Murphy and M. D. Wyatt *Cytotoxicity Small* 2005, 1(3), 325–327,
7 E.G. Victor, P. C.L. Silveira, J. C. Possato, G.L. da Rosa, U. B. Munari, C. T. de Souza, R. A. Pinho, L. da Silva, E.L. Streck and M. M.S. *Journal of Nanobiotechnology* 2012, 10, 11-16.

8 P. Podsiadlo, V. A. Sinani, J. H. Bahng, N.W.S. Kam, J. Lee, and N. A. Kotov. *Langmuir* 2008, 24, 568-574

9 J.G. Leu, S.A. Chen, H.M. Chen, W.M. Wu, C.F. Hung, Y.D. Yao, C.S. Tu and Y.J. Liang. *Nanomedicine: Nanotechnology, Biology, and Medicine* 2012, 8, 767–775

10 S. A.Chena, H.M. Chena, Y. D. Yaob, C. F. Hungc, C.S. Tub and Y.J. Lianga. *European Journal of Pharmaceutical Sciences* 2012, 47, 5, 875–883

11 Z.U. Haq, F. Ali, S.U. Khan and I. Ali *Mediterranean Journal of Chemistry* 2011, 1, 64-69.

12 J.A. Blair, P.A. Ongley, J. Chiswell, and M.H.G. Griffiths *Phytochemistry* 1970, 9(3), 671-677

13 K. M. Ogihara, K. Higa, and T. Suga. *Phytochemistry* 1987, 26, 783-787.

14 P. Sharma, Y.K. Gupta, M.C. Sharma and M.P. Dobhalm *Indian Journal of Chemistry* 2010, 49B, 374-378

15 J.Y. Choi , M. Na, I.H. Hwang and S. H. Lee. *Molecules* 2009, 14, 266-272.

16 G. A. Reza and E. H. Saeidnia *Journal of Pharmaceutical Research* 2011, 10(2), 247-251.

17 J. Wen, H. Shi, Y. Liu, K. Zan, Y. Zhou, Y. Chen, P. Tu and Z.Z. Zazhi. *Chinese Journal of Materia Medica* 2010, 35(14), 1827-1830.

18 S. M.M. Rahman, Z. A. Mukta and M. A. Hossain. *Asian Journal of Food and Agro-Industry* 2009, 2(01), 39-43.

19 F.D. Gunstone, L. K. Jie, and R.T. Wall *Chemistry and Physics of Lipids* 1993, 65, 155-160.

20 I. K. Makhija, H. Vignesh, K. S. Chandrashekar, L. Richard and K.S. Prasanna *Archives of Applied Science Research* 2010, 2(6), 344-348.

21 M.H. Masoodi, B. Ahmed, S.A. Khan and M.Y. Shah *International Research Journal Pharmacy* 2010, 1(1), 337-341.

22 S. L. Helfand, J.Werkmeister, and J.C. Roder. *The Journal of Experimental Medicine,* 1982, 156, 492-505.

23 D. Buso, J. Pacifico, A. Martucci, and P. Mulvaney *Advanced Functional Materials.* 2007, 17, 347-354.

24 J. Y. Song, H. K. Jang and B.S. Kim. *Process Biochemistry* 2009, 44, 1133-1138

25 S. T. Hussain, M. Iqbal, M. Mazha. *Journal of Nanoparticle Research.* 2009, 11, 1383–1391

26 B. Fultz, and J. Howe *Transmission Electron Microscopy and Diffractometry of Materials*. Berlin; New York: Springer, 2002. Print.

27 S. Link and M. A. El-Sayed. *Journal of Physical Chemistry B.* 1999, 103, 4212-4217.

28 M. Pavlin and V. B. Bregar *Digest Journal of Nanomaterials and Biostructures.* 2012, 7, 1389-1400.

Au particles capped with scopoletin, isolated from *Artemisia roxburghiana* by column chromatography, show no change in NO inhibitory activity and inhibition of the oxidative burst of reactive oxygen species (ROS) in whole blood phagocytes and isolated neutrophils is enhanced by three times when compared to pure Scopoletin.